Thermochromism of Polydiacetylenes Containing Robust 2D Hydrogen Bond Network of Naphthylmethylammonium Carboxylates

Satoshi Dei, Tomoyo Shimogaki, and Akikazu Matsumoto*

Department of Applied Chemistry, Graduate School of Engineering, Osaka City University, Sugimoto, Sumiyoshi-ku, Osaka 558-8585, Japan

Received April 14, 2008; Revised Manuscript Received June 18, 2008

ABSTRACT: We investigated the molecular packing structure and the solid-state polymerization behavior of diacetylene compounds containing a naphthylmethylammonium carboxylate group in the side chain, which forms robust and two-dimensional hydrogen bond networks. The resulting polydiacetylenes (PDAs) showed thermochromic behaviors dependent on the structure of the substituents in the side chain. The maximum wavelength of the absorption bands in the UV−vis spectra of the poly(*m,0*-DA-Naph)s, which were obtained by the polymerization of the 1-naphthylmethylammonium 2,4-alkadiynoates ($m = 4-13$, 16), shifted to a longer wavelength region with an increase in the alkyl chain length of the side chain. The poly(*m,0*-DA-Naph)s showed a reversible color change upon heating in a temperature range wider than that for poly(1-naphthylmethylammonium 10,12-pentacosadiynoate) [poly(*12,8*-DA-Naph)] due to the different position of the two-dimensional hydrogen bond network supporting the chain structures in the solid state. We further investigated the structure and chromatic properties of PDAs containing the phenylene substituent groups that are directly connected to the conjugating main chain. Eventually, we found the occurrence of the solid-state polymerization of the 4-carboxyphenyl-substituted diacetylenes as not only naphthylmethylammonium salts (*m,Ph*-DA-Naphs, where $m = 8$, 10, 12, and 16), but also precursor carboxylic acid derivatives (*m,Ph*-DA-CO_2Hs). The poly(*16,Ph*-DA-Naph)s showed a reversible color change upon heating, but the mechanism was different from that of the other PDAs. The thermochromism of poly(*16,Ph*-DA-Naph) included the conformational changes in the aromatic substituent and the conjugating backbone structure.

Introduction

Over the past decades, the eminent properties of conjugated polymers,[1] such as electrical conductivity,[2] use as organic light-emitting diodes,[3] third-order nonlinear optical properties,[4] and chemical or biochemical sensing,[5] have attracted great attention. Especially, materials changing their structures and properties in response to external stimuli or environmental perturbations are important for various applications. Polydiacetylenes (PDAs), one of the conjugated polymers, are obtained by the solid-state polymerization of diacetylene monomers (DAs) as shown in Scheme 1, and have been investigated as key materials for chemical sensing due to their intrinsic blue-to-red color change as well as the fluorescence property.[6–8] Any external stimuli, such as temperature, solvents, ions, pH, mechanical stress, and the binding of specific chemical or biological targets, are adopted as triggers for the chromatic transition of the PDA. The most typical example of applications of PDAs is biochemical sensing as vesicles or thin films using their fluorescence signal, which can be released by a specific molecular recognition event.[9] For example, when the vesicle containing a receptor-binding site is incubated with influenza virus, it displays a drastic color change from blue to red in response to pathogen binding at the interface.[10] Numerous PDA liposomes and films have been developed for the optical detection of small molecules, protein, toxins, antibodies, and so on,[6] since the pioneering work by Charych et al. A reversible color change is often required as characteristic for a wider range of applications, but most PDA chromatic transitions actually occur in an irreversible fashion. Previously, it was reported that Langmuir−Blodgett (LB) membranes of poly(10,12-pentacosadiynoic acid) [poly(*12,8*-DA)] and its cadmium salt derivative exhibit a partly reversible color change between an initial blue and an intermediate purple ones with a thermally distorted structure at a temperature below 50 °C, followed by an irreversible change to the red one upon further heating.[11] After the polymer backbone has a disordered structure, it is difficult to recover its original and highly ordered conformation. When the PDAs include any strong interaction in the side chain, it is expected to exhibit a reversible color change over a wider temperature range. Ahn and Kim et al.[12] have demonstrated the thermally stimulated and pH-stimulated reversible Langmuir−Scheffer films, which exhibit a continuous color change between blue and purple. They demonstrated that hydrogen bonding and aromatic interactions are essentially important for the recovery of the original conformation of the PDA chains after removing the thermal stimulus. They also reported that the blue polymer was stable up to 140 °C without a color change due to strong ladderlike interactions by hydrogen bonding and aromatic interaction when the bola-amphiphilic structure was introduced.[13] Lu et al.[14,15] reported the thermochromism of PDA/silica nanocomposites, in which the side chains of the PDAs are covalently connected to the inorganic silica frameworks. These nanocomposites demonstrate a chromatic change from blue to red at 90 °C, and this color change was reversible below 113 °C. At a higher temperature, the color turned yellow at 150 °C and was no longer reversible. Recently, Dautel et al.[16] reported the thermochromism of PDA organogels containing a urea moiety. A highly ordered and blue gel was obtained by the kinetically controlled solid-state polymerization which irreversibly turned purple upon heating. The blue gel has steric hindrance in its side chains and the strain can be thermodynamically released during the heating. This relaxation process is irreversible.

Other conjugated materials, such as polyacetylenes,[17] polythiophenes,[18] poly(phenylene vinylene)s,[19] polyanilines,[20] and polysilanes,[21] also exhibit reversible chromism against external stimuli, similar to PDAs. In each conjugated polymer, the conformation of the main chain and the electronic properties of the π- or σ-electron are correlated to the chromic behaviors. The color change in the blue and the red forms of the PDAs

* Corresponding author. E-mail: matsumoto@a-chem.eng.osaka-cu.ac.jp.

10.1021/ma800824s CCC: $40.75
Published on Web 07/29/2008

Scheme 1

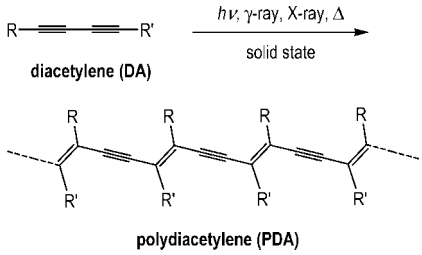

Scheme 2

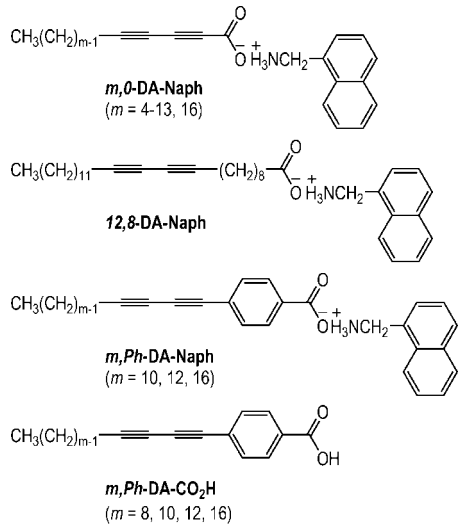

has been discussed from various points of view,[22] and some spectroscopic studies revealed that the color change is induced by a conformational change in the polymer's ene−yne backbone with the different π-electron structures and intermolecular interactions.[23,24] The conformational change is sensitively coupled to the pendant side chain conformation, and a slight rotation around the single bond may cause a significant change in the chromic property of the polymers.

We have previously reported the topochemical polymerization principles and the design of the monomer stacking using supramolecular synthons for the polymerization of 1,3-diene monomers.[25] The most sophisticated molecules included the naphthylmethylammonium group as the countercation of diene carboxylates.[26,27] This group is appropriate for the rational design and the control of the arrangement of monomer molecules in the crystals. Primary ammonium carboxylates have great potential as supramolecular synthons to produce robust 2D hydrogen bond networks. The polarized hydrogen bond formed between the primary ammonium cations and carboxylate anions, which act as triple hydrogen bond donors or acceptors, respectively, makes 1D ladder-type or 2D sheet-type hydrogen bond networks. Moreover, the naphthalene rings effectively support the construction of a columnlike structure to densely pack the monomer molecules in the crystals due to their herringbone-type stacking through π/π and CH/π interactions. We now describe the solid-state polymerization behavior of DAs containing a naphthylmethylammonium carboxylate group in the side chain (*m,0*-DA-Naphs and *12,8*-DA-Naph), in which robust 2D hydrogen bond networks are included. The chemical structures of the DA monomers used in the present study are shown in Scheme 2. The resulting PDAs display a thermochromism depending on the structure of the alkyl substituents and spacers in the side chain. In order to further discuss the conjugating effect of the side chain group, we investigated the structure and chromatic properties of PDAs containing phenylene groups that are directly connected to the conjugating main chain. Eventually, we found the solid-state polymerization of the 4-carboxyphenyl-substituted DA monomers as not only naphthylmethylammonium salts (*m,Ph*-DA-Naphs), but also precursor carboxylic acid derivatives (*m,Ph*-DA-CO_2Hs). The electronic structures of the obtained PDAs were characterized and compared to the other PDAs.

Scheme 3

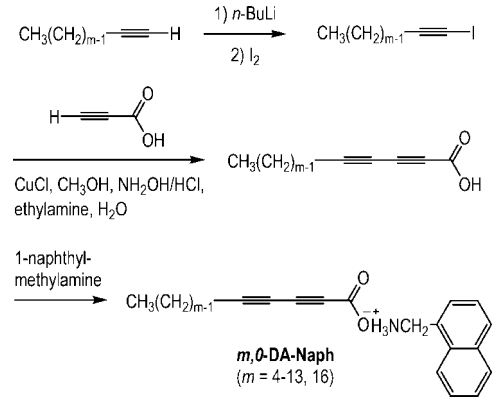

Experimental Section

General Procedures. The NMR spectra were recorded using a JEOL JMN A400 spectrometer in CD_3OD, $CDCl_3$, or DMSO-d_6. The number-average molecular weight (M_n), weight-average molecular weight (M_w), and polydispersity (M_w/M_n) were determined by gel permeation chromatography (GPC) in tetrahydrofuran (THF) as the eluent using a Tosoh CCPD RE-8020 system and calibration with standard polystyrenes. The FT-IR spectra were recorded using a JASCO FT/IR 430 spectrometer equipped with a JASCO Intron IRT-30 infrared microscope and a Mettler-Toledo FP900 temperature controller. The wide-angle X-ray diffraction data were collected using a Rigaku X-ray diffractometer RINT-Ultima 2100 with Cu Kα radiation (λ = 1.5418 Å). The thermogravimetric analysis (TG) was carried out using a Seiko TG/DTA 6200 in a nitrogen stream at the heating rate of 10 °C/min. The onset temperature of decomposition (T_{init}) was determined as the temperature at which a 5% weight loss was observed. The UV−vis spectra were recorded using a JASCO V-550 spectrophotometer at ambient temperature for the PDA solutions. The UV−vis diffusion reflectance spectra were also recorded for the solid samples according to the similar method using an integrating sphere attachment and the $MgSO_4$ powder. The temperature-dependent visible absorption spectra of the solid samples were recorded using a Nikon ECLIPSE E600 POL optical microscope equipped with a Hamamatsu PMA-11 detector and a Mettler-Toledo FP900 temperature controller.

Monomer Synthesis. 1-Naphthylmethylammonium 10,12-pentacosadiynoate (12,8-DA-Naph) was prepared from the commercially available 10,12-pentacosadiynoic acid (Alfa Aesear, Tokyo) and 1-naphthylmethylamine (Aldrich) in chloroform and quantitatively isolated by precipitation with a large amount of *n*-hexane. After the filtration and drying in vauo, *12,8*-DA-Naph was obtained as a colorless powder.

12,8-DA-Naph. Colorless powder, T_{init} = 164.2 °C; ^{1}H NMR (400 MHz, CD_3OD and $CDCl_3$) δ 8.05−7.32 (m, Naph, 7H), 4.34 (s, Naph-CH_2, 2H), 2.33−2.22 (m, CH_2, 6H), 1.63−1.26 (m, CH_2, 32H), 0.88 (t, J = 7.2 Hz, CH_3, 3H). 2θ (Cu Kα) = 2.84, 5.78, 7.23, 8.69, 10.14, 11.61, 14.54, 16.00, 17.48, 18.90, 21.46, 21.88, 22.58, 23.00, 24.12, 24.88, 26.36, 30.88, 36.94, and 38.46 deg.

The 1-naphthylmethylammonium 2,4-alkadiynoates (*m,0*-DA-Naphs) were prepared from the corresponding 2,4-alkadiynoic acids (*m,0*-DA-CO_2Hs) and 1-naphthylmethylamine, similar to the method for the synthesis of 12,8-DA-Naph. The *m,0*-DA-CO_2Hs were prepared by the Cadiot−Chodkiezicz coupling reaction[28] (Scheme 3). A typical example of this procedure is as follows.

Synthesis of 1-Iodo-1-tetradecyne. To a four-necked flask equipped with a dropping funnel, 1-tetradecyne (5 g, 0.026 mol) and 30 mL of THF were added under an argon stream. The solution was cooled to 0 °C, and then 19.7 mL of *n*-butyllithium (1.57 mol/L in *n*-hexane, Kanto Kagaku) was added using a syringe. Iodine (7.8 g) in 30 mL of THF was added at room temperature and the mixture was further stirred for 2 h. The excess *n*-butyllithium was treated with 20 mL of water. The whole mixture was extracted several times with a total of 1 L of *n*-hexane. The extracts were then dried over Na_2SO_4. The product was purified by silica gel column chromatography with *n*-hexane. 1-Iodo-1-tetradecyne was obtained as a slightly red liquid by the evaporation of the solvent. The yield was 91%.

1-Naphthylmethylammonium 2,4-Heptadecadiynate (*12,0*-DA-Naph). To the 70% aqueous solution of ethylamine (19 mL) was added 9 mL of distilled water, hydroxylamine hydrochloride (2.34 g), copper(I) chloride (350 mg) in a 200 mL four-necked flask under an argon stream. The solution was cooled to 0 °C, and then was dropwise added propiolic acid (1.96 g) in 30 mL of THF. 1-Iodo-1-tetradecyne (7.5 g) in 30 mL of THF was further added over 30 min. The temperature of the reaction mixture was then raised to room temperature, and the suspension was stirred overnight under a nitrogen stream. The red reaction mixture was filtered, and the solid was washed with 20 mL of THF. The solvent was evaporated, and a 1 mol/L HCl aqueous solution was added until the solution became acidic. The solution was extracted several times with a total of 1 L of diethyl ether, and the extracts were dried over Na_2SO_4. After filtration, the solvent was removed by evaporation. The crude 2,4-heptadecadiynic acid was obtained in a 64% yield, dissolved in methanol together with 1-naphthylmethylamine, and then poured into a large amount of diethyl ether. By filtration, *12,0*-DA-Naph was quantitatively isolated as a colorless powder. The yields of *m,0*-DA-Naph are shown as yield of the precursor acids. The *m,0*-DA-Naph monomers decomposed over 100 °C, thus showing no melting point.

1-Naphthylmethylammonium 2,4-Nonadiynate (4,0-DA-Naph). Yield 50%, colorless powder, T_{init} = 112.1 °C; ^{1}H NMR (400 MHz, CD_3OD) δ 8.09−7.54 (m, Naph, 7H), 4.62 (s, NaphCH_2, 2H), 2.31 (t, J = 7.2 Hz, CH_2, 2H), 1.51−1.41 (m, CH_2, 4H), 0.92 (t, J = 7.2 Hz, CH_3, 3H); ^{13}C NMR (100 MHz, CD_3OD) δ 157.94 (C═O), 133.18, 130.08, 128.91, 128.06, 127.94, 126.49, 126.13, 125.24, 124.31, and 121.39 (Naph), 82.45, 70.48, 63.59, and 63.24 (C≡C), 39.17 (Naph*C*H_2), 29.10, 20.71, and 17.44 (CH_2), 11.69 (CH_3); IR (KBr) 2243 ($\nu_{C\equiv C}$) cm^{-1}. Anal. Calcd for $C_{19}H_{21}N_1O_2$: C, 77.09; H, 6.67; N, 4.96%. Found: C, 77.26; H, 7.17; N, 4.74%. 2θ (Cu Kα) = 2.82, 5.68, 8.54, 11.40, 14.28, 15.78, 16.02, 16.84, 17.16, 19.62, 20.06, 21.66, 23.00, 23.30, 24.36, 24.86, 25.50, 25.87, 27.20, 28.38 30.28, and 37.76.

1-Naphthylmethylammonium 2,4-Decadiynate (5,0-DA-Naph). Yield 88%, colorless powder, T_{init} = 135.0 °C; ^{1}H NMR (400 MHz, CD_3OD) δ 8.11−7.52 (m, Naph, 7H), 4.62 (s, NaphCH_2, 2H), 2.31 (t, J = 7.2 Hz, CH_2, 2H), 1.52 (m, CH_2, 2H), 1.35 (m, CH_2, 4H), 0.91 (t, J = 7.2 Hz, CH_3, 3H); ^{13}C NMR (100 MHz, CD_3OD) δ 160.14 (C═O), 135.45, 132.34, 131.12, 130.13, 128.72, 128.33, 127.54, 126.52, and 123.63 (Naph), 84.90, 72.67, 65.81, and 65.36 (C≡C), 41.29 (Naph*C*H_2), 30.09, 28.91, 23.17, and 19.83 (CH_2), 14.29 (CH_3). 2θ (Cu Kα) = 2.64, 5.34, 8.04, 10.74, 13.46, 16.14, 18.56, 22.42, 23.14, 24.60, 25.24, 26.32, 27.14, 29.22, 29.76, 30.54, 32.68, and 38.34 deg.

1-Naphthylmethylammonium 2,4-Undecadiynate (6,0-DA-Naph). Yield 97%, colorless powder, T_{init} = 134.8 °C; ^{1}H NMR (400 MHz, CD_3OD) δ 8.12−7.52 (m, Naph, 7H), 4.62 (s, NaphCH_2, 2H), 2.30 (t, J = 6.8 Hz, CH_2, 2H), 1.51−1.26 (m, CH_2, 8H), 0.90 (t, J = 6.8 Hz, CH_3, 3H)); ^{13}C NMR (100 MHz, CD_3OD) δ 160.13 (C═O), 135.39, 132.33, 131.02, 130.40, 130.08, 128.69, 128.29, 127.49, 126.52, and 123.69 (Naph), 84.84, 72.72, 65.77, and 65.38 (C≡C), 41.32 (Naph*C*H_2), 32.37, 29.53, 29.17, 23.56, and 19.86 (CH_2), 14.35 (CH_3). Anal. Calcd for $C_{21}H_{25}N_1O_2$: C, 77.62; H, 7.38; N, 4.26%. Found: C, 77.98; H, 7.79; N, 4.33%. 2θ (Cu Kα) = 2.54, 5.10, 7.66, 10.22, 15.36, 15.86, 16.32, 18.04, 20.00, 20.38, 20.82, 21.06, 22.10, 22.80, 23.28, 24.54, 25.00, 25.24, 25.80, 27.54, 30.30, and 30.68 deg.

1-Naphthylmethylammonium 2,4-Dodecadiynate (7,0-DA-Naph). Yield 90%, colorless powder, T_{init} = 133.8 °C; ^{1}H NMR (400 MHz, CD_3OD) δ 8.12−7.52 (m, Naph, 7H), 4.62 (s, NaphCH_2, 2H), 2.30 (t, J = 6.8 Hz, CH_2, 2H), 1.51−1.28 (m, CH_2, 10H), 0.89 (t, J = 6.8 Hz, CH_3, 3H); ^{13}C NMR (100 MHz, CD_3OD) δ 160.11 (C═O), 135.41, 132.33, 131.07, 130.34, 130.10, 128.72, 128.31, 127.51, 126.52, and 123.67 (Naph), 84.80, 72.71, 65.74, and 65.38 (C≡C), 41.32 (Naph*C*H_2), 32.86, 29.82, 29.21, 23.64, and 19.85 (CH_2), 14.39 (CH_3). Anal. Calcd for $C_{22}H_{27}N_1O_2$: C, 78.78; H, 7.72; N, 3.96%. Found: C, 78.30; H, 8.07; N, 4.15%. 2θ (Cu Kα) = 2.40, 4.82, 7.24, 9.66, 14.52, 15.74, 16.96, 19.88, 20.18, 20.72, 21.64, 22.74, 23.02, 24.30, 24.70, 25.36, 26.80, 28.88, 30.38, and 36.54 deg.

1-Naphthylmethylammonium 2,4-Tridecadiynate (8,0-DA-Naph). Yield 78%, colorless powder, T_{init} = 126.4 °C; ^{1}H NMR (400 MHz, CD_3OD) δ 8.11−7.52 (m, Naph, 7H), 4.62 (s, NaphCH_2, 2H), 2.29 (t, J = 7.2 Hz, CH_2, 2H), 1.51−1.28 (m, CH_2, 12H), 0.88 (t, J = 7.2 Hz, CH_3, 3H); ^{13}C NMR (100 MHz, CD_3OD) δ 159.02 (C═O), 135.32, 132.28, 131.11, 130.79, 130.25, 128.77, 128.33, 127.41, 126.49, and 123.64 (Naph), 82.71, 72.25, 65.44, and 65.43 (C≡C), 40.25 (Naph*C*H_2), 33.02, 30.81, 30.55, 29.91, 29.22, 22.94, and 19.82 (CH_2), 13.81 (CH_3). Anal. Calcd for $C_{23}H_{29}N_1O_2$: C, 78.73; H, 7.99; N, 3.99%. Found: C, 78.59; H, 8.32; N, 3.99%. 2θ (Cu Kα) = 2.26, 4.54, 6.84, 9.12, 13.68, 15.92, 17.16, 18.30, 19.40, 19.80, 20.70, 20.90, 22.52, 22.86, 24.22, 24.50, 25.04, 25.86, 27.60, 27.84, and 30.18 deg.

1-Naphthylmethylammonium 2,4-Tetradecadiynate (9,0-DA-Naph). Yield 89%, colorless powder, T_{init} = 127.9 °C; ^{1}H NMR (400 MHz, CD_3OD) δ 8.11−7.52 (m, Naph, 7H), 4.62 (s, NaphCH_2, 2H), 2.30 (t, J = 7.2 Hz, CH_2, 2H), 1.53−1.29 (m, CH_2, 14H), 0.89 (t, J = 7.2 Hz, CH_3, 3H); ^{13}C NMR (100 MHz, CD_3OD) δ 160.10 (C═O), 135.42, 132.34, 131.07, 130.35, 130.11, 128.72, 128.31, 127.51, 126.52, and 123.66 (Naph), 84.74, 72.45, 65.71, and 65.40 (C≡C), 41.34 (Naph*C*H_2), 33.02, 30.58, 30.38, 30.16, 29.87, 29.22, 23.72, and 19.86 (CH_2), 14.44 (CH_3). Anal. Calcd for $C_{24}H_{31}N_1O_2$: C, 79.17; H, 8.21; N, 3.73%. Found: C, 78.86; H, 8.55; N, 3.83%. 2θ (Cu Kα) = 2.18, 4.36, 6.56, 8.74, 13.10, 15.32, 15.82, 17.52, 19.90, 22.00, 23.00, 23.60, 24.26, 24.82, 25.40, 26.44, 27.08, 28.66, 30.30, and 37.74 deg.

1-Naphthylmethylammonium 2,4-Pentadecadiynate (10,0-DA-Naph). Colorless powder, T_{init} = 128.9 °C; ^{1}H NMR (400 MHz, CD_3OD) δ 8.12−7.52 (m, Naph, 7H), 4.61 (s, NaphCH_2, 2H), 2.31 (t, J = 7.2 Hz, CH_2, 2H), 1.50−1.30 (m, CH_2, 16H), 0.88 (t, J = 6.8 Hz, CH_3, 3H); ^{13}C NMR (100 MHz, CD_3OD) δ 158.21 (C═O), 135.43, 132.34, 131.06, 130.51, 130.12, 128.67, 128.31, 127.52, 126.53, and 123.65 (Naph), 82.69, 72.71, 65.67, and 65.41 (C≡C), 41.40 (Naph*C*H_2), 33.07, 30.69, 30.64, 30.46, 30.16, 29.89, 29.24, 23.74, and 19.86 (CH_2), 14.45 (CH_3). Anal. Calcd for $C_{25}H_{33}N_1O_2$: C, 79.18; H, 8.39; N, 3.65%. Found: C, 79.11; H, 8.76; N, 3.69%. 2θ (Cu Kα) = 4.16, 6.26, 8.34, 12.52, 15.80, 16.36, 16.72, 17.72, 18.01, 19.84, 20.32, 20.78, 21.02, 21.50, 22.84, 24.22, 24.64, 25.00, 26.26, 30.48, and 36.6 deg.

1-Naphthylmethylammonium 2,4-Hexadecadiynate (11,0-DA-Naph). Yield 89%, colorless powder, T_{init} = 120.7 °C; ^{1}H NMR (400 MHz, CD_3OD) δ 8.12−7.52 (m, Naph, 7H), 4.62 (s, NaphCH_2, 2H), 2.30 (t, J = 7.2 Hz, CH_2, 2H), 1.53−1.17 (m, CH_2, 18H), 0.89 (t, J = 7.2 Hz, CH_3, 3H); ^{13}C NMR (100 MHz, CD_3OD) δ 160.10 (C═O), 135.42, 132.34, 131.09, 130.36, 130.12, 128.72, 128.32, 127.53, 126.52, and 123.65 (Naph), 84.72, 72.73, 65.69, and 65.41 (C≡C), 41.34 (Naph*C*H_2), 33.07, 30.72, 30.62, 30.46, 20.16, 29.88, 29.23, 23.73, and 19.86 (CH_2), 14.44 (CH_3). Anal. Calcd for $C_{26}H_{35}N_1O_2$: C, 79.62; H, 8.59; N, 3.41%. Found: C, 79.34; H, 8.96; N, 3.56%. 2θ (Cu Kα) = 4.00, 6.02, 8.02, 12.04, 16.08, 18.32, 19.66, 19.96, 20.38, 21.62, 22.84, 23.32, 24.26, 24.48, 25.64, 25.92, 28.38, and 36.70 deg.

1-Naphthylmethylammonium 2,4-Heptadecadiynate (12,0-DA-Naph). : Yield 64%, colorless powder, T_{init} = 145.0 °C; ^{1}H NMR (400 MHz, CD_3OD) δ 8.10−7.53 (m, Naph, 7H), 4.62 (s, NaphCH_2,

Scheme 4

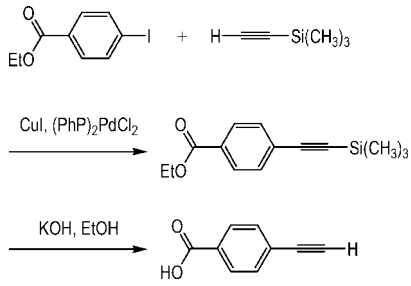

2H), 2.31 (t, J = 6.8 Hz, CH_2, 2H), 1.52−1.29 (m, CH_2, 20H), 0.90 (t, J = 6.8 Hz, CH_3, 3H);^{13}C NMR (100 MHz, CD_3OD) δ 160.08 (C═O), 141.52, 135.43, 131.11, 130.14, 129.00, 128.70, 128.33, 127.54, 126.52, and 123.62 (Naph), 84.64, 72.76, 65.62, and 65.42 (C≡C), 41.38 (Naph*C*H_2), 33.09, 30.77, 30.72, 30.64, 30.49, 30.18, 29.88, 29.24, 23.74, and 19.84 (CH_2), 14.45 (CH_3). Anal. Calcd for $C_{27}H_{37}N_1O_2$: C, 79.65; H, 8.81; N, 3.33%. Found: C, 79.56; H, 9.15; N, 3.44%. 2θ (Cu Kα) = 3.82, 5.74, 7.66, 11.52, 13.46, 15.38, 17.50, 19.54, 19.90, 20.74, 21.20, 22.08, 23.48, 24.20, 24.46, 24.86, 25.34, 26.60, 27.12, 30.16, and 37.09 deg.

1-Naphthylmethylammonium 2,4-Octadecadiynate (13,0-DA-Naph). Yield 99%, colorless powder, T_{init} = 126.1 °C; ^{1}H NMR (400 MHz, CD_3OD) δ 8.12−7.52 (m, Naph, 7H), 4.62 (s, NaphCH_2, 2H), 2.31 (t, J = 7.2 Hz, CH_2, 2H), 1.52−1.29 (m, CH_2, 22H), 0.89 (t, J = 7.2 Hz, CH_3, 3H);^{13}C NMR (100 MHz, CD_3OD) δ 160.10 (C═O), 135.43, 132.35, 131.07, 130.46, 130.13, 128.70, 128.32, 127.53, 126.53, and 123.66 (Naph), 84.70, 72.74, 65.68, and 65.42 (C≡C), 41.39 (Naph*C*H_2), 33.09, 30.79, 30.76, 30.72, 30.63, 30.48, 30.17, 29.89, 29.24, 23.74, and 19.86 (CH_2), 14.45 (CH_3). Anal. Calcd for $C_{28}H_{39}N_1O_2$: C, 79.80; H, 9.02; N, 3.20%. Found: C, 79.76; H, 9.32; N, 3.32%. 2θ (Cu Kα) = 3.70, 7.38, 11.14, 14.84, 15.86, 16.74, 18.32, 20.02, 20.50, 21.10, 21.60, 22.95, 24.32, 24.86, 25.88, 30.16, 30.64, 32.12, and 37.18 deg.

1-Naphthylmethylammonium 2,4-Henicosadiynate (16,0-DA-Naph). Colorless powder, T_{init} = 144.1 °C; ^{1}H NMR (400 MHz, CD_3OD) δ 8.09−7.52 (m, Naph, 7H), 4.59 (s, NaphCH_2, 2H), 2.31 (t, J = 7.2 Hz, CH_2, 2H), 1.56−1.29 (m, CH_2, 28H), 0.89 (t, J = 6.8 Hz, CH_3, 3H); ^{13}C NMR (100 MHz, CD_3OD) δ 158.37 (C═O), 139.56, 131.14, 130.53, 129.02, 128.54, 128.34, 127.54, 126.50, 125.41, and 123.54 (Naph), 85.57, 73.06, 65.61, and 65.53 (C≡C), 41.50 (NaphCH_2), 33.01, 30.67, 30.52, 30.36, 30.09, 29.85, 29.26, 23.64, and 19.88 (CH_2), 14.31 (CH_3). Anal. Calcd for $C_{31}H_{45}N_1O_2$: C, 80.01; H, 9.37; N, 2.91%. Found: C, 80.29; H, 9.78; N, 3.02%. 2θ (Cu Kα) = 3.28, 6.64, 9.96, 13.36, 15.78, 16.10, 16.72, 17.12, 18.80, 20.06, 20.66, 21.74, 23.00, 24.38, 24.84, 25.62, 26.98, 28.36, 30.28, and 37.42 deg.

The *m,Ph*-DA-CO_2Hs were prepared by the Cadiot−Chodkiezicz coupling reaction[28] of the corresponding 1-iodo-1-alkynes with (4-carboxyphenyl)acetylene, which was obtained by the Sonogashira coupling reaction.[28] The ammonium salts were prepared by the reaction with 1-naphthylmethylamine in methanol.

Synthesis of (4-Carboxyphenyl)acetylene.[29] According to Scheme 4, to the mixture of ethyl 4-iodobenzoate (12.5 g, 0.045 mol), bis(triphenylphosphine)palladium dichloride (125 mg), triphenylphosphine (190 mg), and copper(I) iodide (210 mg) in triethylamine (150 mL) was added (trimethylsilyl)acetylene (9.6 mL). The reaction mixture was stirred overnight under nitrogen at room temperature, and then the triethylamine was evaporated under reduced pressure. The residue was chromatographed on silica gel with a mixture of *n*-hexane and ethyl acetate in 1/2 volume ratio. After the solvent was removed under reduced pressure, the resulting ethyl [4-(trimethylsilyl)ethynyl]benzoate was dissolved in 30 mL of ethanol, an excess amount of KOH (5.1 g) was added to the solution at room temperature, and then stirred overnight. After the reaction, the solution was washed with 500 mL of diethyl ether, and the aqueous layer was acidified with conc. HCl aqueous solution. The precipitated solid was extracted several times with a total of 1 L of diethyl ether, and dried over Na_2SO_4. The

Scheme 5

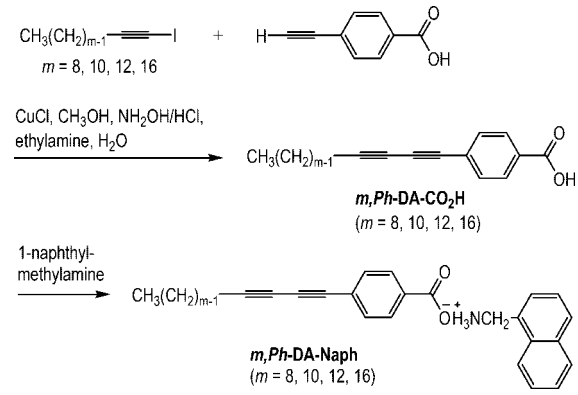

(4-carboxyphenyl)acetylene was obtained as orange crystals by the evaporation of the solvent. The yield was 50%.

Synthesis of 1,3-Hexadecadiynyl-4-benzoic Acid (*12,Ph*-DA-CO_2H). As shown in Scheme 5, to 9.6 mL of the 70% ethylamine aqueous solution, 5 mL of distilled water, hydroxylamine hydrochloride (1.2 g), and copper(I) chloride (0.18 g) in a 200 mL four-necked flask under an argon stream was dropwise added (4-carboxyphenyl)acetylene (2.02 g) in 30 mL of THF over 10 min, and then 1-iodo-1-tetradecyne (4.8 g, 0.012 mol) in 30 mL of THF over 30 min. After the solution was stirred overnight, the solvent was evaporated, and the HCl aqueous solution (1 mol/L) was added until the solution became acidic. The solution was extracted with 1 L of diethyl ether, and then the solvent was removed. The crude residue was purified by recrystallization from a mixture of THF and methanol. The *12,Ph*-DA-CO_2H was obtained as a colorless powder in the yield of 89%.

1,3-Dodecadiynyl-4-benzoic Acid (8,Ph-DA-CO_2H). Yield 32%; colorless powder, T_{init} = 246.5 °C; ^{1}H NMR (400 MHz, DMSO-d_6) δ 13.20 (s, CO_2H, 1H), 7.91 and 7.62 (d, J = 8.4 Hz, C_6H_4, 4H), 2.43 (t, J = 6.8 Hz, C≡CCH_2, 2H), 1.50 (q, C≡CCH_2CH_2, 2H) 1.35−1.25 (m, CH_2, 10H), 0.85 (t, J = 7.2 Hz, CH_3, 3H); ^{13}C NMR (100 MHz, DMSO-d_6) δ 116.52 (CO_2H), 132.51, 131.15, 129.5, and 125.2 (C_6H_4), 87.48, 76.66, 73.78, and 64.53 (C≡C), 31.21, 28.54, 28.38, 28.24, 27.50, 22.05, and 18.69 (CH_2), 13.94 (CH_3); IR (KBr) 2411 ($\nu_{C\equiv C}$), 1688 ($\nu_{C=O}$) cm^{-1}. Anal. Calcd for $C_{19}H_{22}O_2$: C, 80.51; H, 7.89%. Found: C, 80.81; H, 7.85%. 2θ (Cu Kα) = 4.78, 8.70, 9.10, 9.58, 10.67, 11.66, 12.96, 13.44, 13.96, 14.34, 17.40, 18.20, 18.96, 19.84, 20.40, 22.16, 23.32, 23.72, 26.68, and 27.82 deg.

1,3-Tetradecadiynyl-4-benzoic Acid (10,Ph-DA-CO_2H). Yield 36%; colorless powder. T_{init} = 273.7 °C; ^{1}H NMR (400 MHz, DMSO-d_6) δ 13.02 (s, CO_2H, 1H), 7.92 and 7.63 (d, J = 8.4 Hz, C_6H_4, 4H), 2.43 (t, J = 6.8 Hz, C'CCH_2, 2H), 1.55−1.26 (m, CH_2, 16H), 0.85 (t, J = 6.8 Hz, CH_3, 3H); ^{13}C NMR (100 MHz, DMSO-d_6) δ 132.54, 129.88, and 125.24 (C_6H_4), 87.38, 76.66, 73.82, and 64.56 (C≡C), 31.21, 28.83, 28.88, 28.77, 28.56, 28.31, 28.16, 27.47, 21.98, and 18.69 (CH_2), 13.79 (CH_3); IR (KBr) 2242 ($\nu_{C\equiv C}$), 1685 ($\nu_{C=O}$) cm^{-1}. Anal. Calcd for $C_{21}H_{26}O_2$: C, 80.92; H, 8.40%. Found: C, 81.25; H, 8.44%. 2θ (Cu Kα) = 2.46, 4.92, 7.38, 14.78, 16.22, 18.08, 19.22, 19.58, 20.06, 20.80, 21.14, 22.42, 24.24, 25.18, 25.50, 25.74, 26.78, 27.28, 28.00, 29.38, 30.02, 33.10, 36.34, and 39.08 deg.

1,3-Hexadecadiynyl-4-benzoic Acid (12,Ph-DA-CO_2H). Yield 89%; colorless powder, T_{init} = 251.8 °C; ^{1}H NMR (400 MHz, DMSO-d_6) δ 13.08 (s, CO_2H, 1H), 7.93 and 7.63 (d, J = 8.4 Hz, C_6H_4, 4H), 2.43 (t, J = 6.8 Hz, C'CCH_2, 2H), 1.55−1.24 (m, CH_2, 20H), 0.85 (t, J = 6.8 Hz, CH_3, 3H); ^{13}C NMR (100 MHz, DMSO-d_6) δ 166.63 (C═O), 132.61, 132.00, 131.37, 129.39, and 125.40 (C_6H_4), 87.59, 76.84, 73.97, and 64.73 (C≡C), 31.41, 29.12, 29.06, 28.96, 28.81, 28.50, 28.34, 27.64, 22.19, and 18.87 (CH_2), 14.02 (CH_3); IR (KBr) 2242 ($\nu_{C\equiv C}$) 1700 ($\nu_{C=O}$), 1683 ($\nu_{C=O}$) cm^{-1}. Anal. Calcd for $C_{23}H_{30}O_2$: C, 81.48; H, 9.01%. Found: C, 81.61; H,

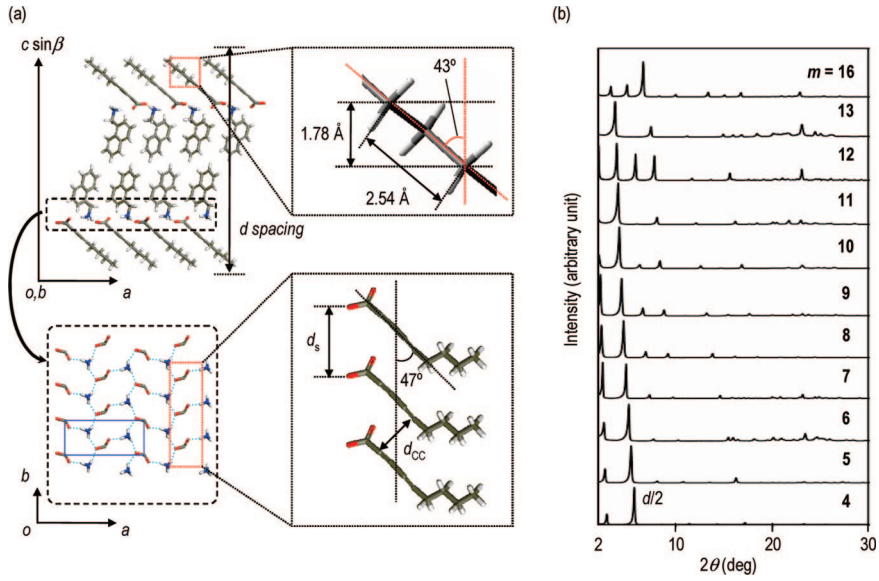

Figure 1. (a) Crystal structure of *4,0*-DA-Naph viewed down along the *b*-axis of the crystals and hydrogen bond network formed in *ab* plane. The tilt angle of the alkyl chains in the side chain against the layer of 2D hydrogen network and monomer stacking structures in a column formed in the direction of the *b*-axis for *4,0*-DA-Naph are also shown. The d_s and d_{CC} values are 4.88 and 3.66 Å, respectively. A blue rectangle indicates a unit for the grid of 2D hydrogen network. (b) Powder X-ray diffraction profiles of *m,0*-DA-Naphs with different alkyl substituents ($m = 4-13$, 16).

8.93%. 2θ (Cu Kα) = 2.24, 4.48, 6.72, 13.44, 19.18, 19.46, 19.98, 20.66, 22.50, 27.16, and 27.72 deg.

1,3-Icosadiynyl-4-benzoic Acid (16,Ph-DA-CO$_2$H). Yield 51%; colorless powder, T_{init} = 283.3 °C; ^{1}H NMR (400 MHz, DMSO-d_6) δ 13.02 (s, CO_2H, 1H), 7.92 and 7.62 (d, J = 8.4 Hz, C_6H_4, 4H), 2.43 (t, J = 6.8 Hz, C≡CCH_2, 2H), 1.55−1.23 (m, CH_2, 28H), 1.49 (t, J = 6.8 Hz, CH_3, 3H); ^{13}C NMR (100 MHz, DMSO-d_6) δ 166.39 (C=O), 132.37, 131.20, 129.39, and 125.22 (C_6H_4), 87.37, 76.65, 73.79, and 64.52 (C≡C), 31.18, 28.91, 28.88, 28.86, 28.81, 28.71, 28.56, 28.25, 28.11, 27.43, 21.95, and 18.67 (CH_2), 13.78 (CH_3); IR (KBr) 2241 ($\nu_{C\equiv C}$) 1703 ($\nu_{C=O}$), 1683 ($\nu_{C=O}$) cm^{-1}. Anal. Calcd for $C_{27}H_{38}O_2$: C, 81.91; H, 9.73%. Found: C, 82.18; H, 9.71%. 2θ (Cu Kα) = 1.90, 3.78, 5.68, 9.48, 11.36, 15.20, 16.20, 19.14, 19.50, 19.92, 20.68, 21.44, 22.52, 23.90, 25.52, 27.11, 27.46, 27.86, and 28.42 deg.

1-Naphthylmethylammonium 1,3-Tetradecadiynyl-4-benzoate (10,Ph-DA-Naph). Colorless powder. ^{1}H NMR (400 MHz, DMSO-d_6) δ 8.16−7.48 (m, Naph and C_6H_4, 11H), 4.45 (s, NaphCH_2, 2H), 2.41 (t, J = 6.8 Hz, C≡CCH_2, 2H), 1.52−1.25 (m, CH_2, 20H), 0.85 (t, J = 7.2 Hz, CH_3, 3H); 2θ (Cu Kα) = 3.62, 5.44, 7.24, 10.88, 12.68, 14.52, 15.42, 16.52, 16.74, 19.20, 20.48, 20.76, 21.58, 22.18, 22.76, 24.36, 24.66, 25.82, 26.10, 27.40, and 30.14 deg.

1-Naphthylmethylammonium 1,3-Hexadecadiynyl-4-benzoate (12,Ph-DA-Naph). Colorless powder; T_{init} = 174.7 °C. ^{1}H NMR (400 MHz, DMSO-d_6) δ 8.17−7.30 (m, Naph and C_6H_4, 11H), 4.21 (s, NaphCH_2, 2H), 2.41 (t, J = 6.8 Hz, C≡CCH_2, 2H), 1.52−1.24 (m, CH_2, 20H), 0.84 (t, J = 7.2 Hz, CH_3, 3H). 2θ (Cu Kα) = 3.44, 6.18, 6.64, 12.40, 12.80, 15.28, 15.90, 17.04, 18.70, 20.14, 20.62, 21.32, 23.32, 24.16, 24.92, 25.36, 27.02, 28.08, 29.90, 30.84, 36.10, 36.64, and 38.24 deg.

1-Naphthylmethylammonium 1,3-Icosadiynyl-4-benzoate (16,Ph-DA-Naph). Colorless powder, T_{init} = 170.6 °C; ^{1}H NMR (400 MHz, CD_3OD) δ 8.05−7.50 (m, Naph, 7H), 3.38 (s, NaphCH_2, 2H) 2.37 (t, J = 6.8 Hz, C≡CCH_2, 2H), 1.60−1.26 (m, CH_2, 28H), 0.88 (t, J = 7.2 Hz, CH_3, 3H); IR (KBr) 2242 ($\nu_{C\equiv C}$) cm^{-1}. 2θ (Cu Kα) = 2.96, 4.40, 5.90, 11.82, 15.64, 16.44, 17.76, 18.06, 20.38, 21.02, 21.48, 21.80, 22.10, 23.34, 24.00, 24.34, 24.88, 26.86, 30.04, and 36.46 deg.

Polymerization Procedures. The photopolymerization of the DA monomers was carried out in the solid state under UV irradiation with a high-pressure mercury lamp (Toshiba SHL-100-2, 100 W) or a low-pressure mercury lamp (AS ONE SLUV-4, 9 W, 254 nm) at a distance of 10 cm. A high-pressure mercury lamp was used unless otherwise noted. The measurements of UV−vis and IR spectra were carried out for the samples after polymerization without the isolation of the polymer. The γ-radiation of *m,Ph*-DA-Naphs and *m,Ph*-DA-CO_2Hs was carried out at a radiation dose of 200 or 1000 kGy (a dose rate of 9.7 kGy/h) using ^{60}Co at the Osaka Prefecture University. The resulting poly(*16,Ph*-DA-Naph) and poly(*m,Ph*-DA-CO_2H)s were isolated as the insoluble part in THF and the polymer yield was gravimetrically determined. The poly(*10,Ph*-DA-Naph) and poly(*12,Ph*-DA-Naph) were partly soluble in THF, provided for the GPC measurement.

Thermochromic Measurements. A polymer solid film was obtained by casting the methanol solution of the *m,0*-DA-Naph monomer on a glass plate and the subsequent UV irradiation for 10 s without isolating the resulting polymer. The surface of the solid film soon became blue during the irradiation. The solid films were used for the measurement of the UV−vis absorption spectrum under temperature control (Figures 4–7). The conversion of the monomer to the polymer was determined on the basis of a decrease in the intensity of the absorption band due to the CC triple bond observed at 2241−2243 cm^{-1} in the IR spectrum. The conversion was approximately 5% under the irradiation conditions used in the present study.

Results and Discussion

Layered Structure of *m,0*-DA-Naph Monomers. The crystal structure of a series of *m,0*-DA-Naph monomers was investigated on the basis of the results of the X-ray single-crystal structure analysis[30] and the powder X-ray diffraction measurement. The carboxylic acid derivatives as precursors, *m,0*-DA-CO_2Hs, are oily when the length of the alkyl substituent is short (m < 9), but all the 1-naphthylmethylammonium salts of the acids were isolated as colorless and crystalline powders independent of the alkyl length. The molecular packing structure of *4,0*-DA-Naph in the crystals is shown in Figure 1a. The monomer molecules are arranged in a columnlike structure with the stacking distance (d_s) and angle of 4.88 Å and 47°, respectively, along the *b*-axis of the crystal. The carbon-to-carbon distance (d_{CC}) for 1,4-propagation during polymerization is 3.66 Å. These stacking parameters are appropriate for the polymerization of the diyne compounds. The stacking structure of the other *m,0*-DA-Naph monomers with larger *m* values was estimated from the interlayer distance (*d*-spacing) determined

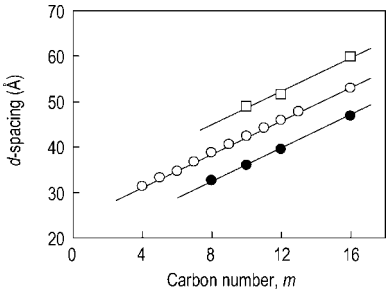

Figure 2. Relationship between the carbon number (m) of the alkyl chain and interlayer distance (d) of the monomer crystals in the series of *m,0*-DA-Naph (○), *m,Ph*-DA-Naph (□), and *m,Ph*-DA-CO_2H (●).

by the powder X-ray diffraction (Figure 1b). The 2θ values for the diffraction of each monomer are shown in Experimental Section. As a result, it was confirmed that the *d*-spacing values linearly increased with an increase in the alkyl-chain length, as shown in Figure 2. The linear relationship between the *m* and *d* values (an increase in the *d*-spacing by 0.89 Å per the carbon number) suggests that alkyl chains have a structure inclined to the lamellar sheets with a tilt angle of 43°. The fiber period of the *m,0*-DA-Naph crystal is 4.88 Å, which is identical to the one of the lattices of a 2D grid (the side lengths are 4.88 and 11.2 Å)[31] for the hydrogen bond networks of the naphthylmethylammonium carboxylate functions. If the alkyl chains perpendicularly stand on the 2D sheet of hydrogen bond networks, the alkyl chains are very loosely packed. For the close packing of the alkyl chains, they are favorably tilted with the angle of 43° in a direction along to *a*-axis. Similar tilt angles were also observed for the other layered crystals of saturated[27] and unsaturated[26] carboxylates coupled with the naphthylmethylammonium countercation, because the 2D hydrogen bond networks consisting of naphthylmethylammonium carboxylates always have the same structure. A similar inclined stacking of the long-alkyl chain compounds is also reported for some other molecular assembly systems including intercalation compounds.[32] No even−odd number effects were observed in a series of *m,0*-DA-Naphs, being similar to the results for the naphthylmethylammonium *n*-alkanoates, in contrast to the frequent appearance of polymorph for the crystals of *n*-parrafins and α,ω-difunctional alkanes with the strong even−odd number effect.[33,34] This is due to the intense power of the naphthylmethylammonium as countercation for the molecular arrangement in the unique 2D grid of the hydrogen bond networks.

Solid-State Polymerization of *m,0*-DA-Naphs. The photopolymerization of the DA monomers was carried out in the solid state under UV irradiation with a high-pressure mercury lamp at ambient temperature at a distance of 10 cm from the surface of the samples. The process of photopolymerization was confirmed by a color change in the appearance of the crystalline powder. That is, the PDA crystals immediately became blue, purple, or red color, depending on the monomer structure and polymerization conditions during the UV irradiation. The maximum wavelength of the absorption band depended on the *m* value. Figure 3a shows the diffusion reflectance spectra of the samples including the resulting poly(*m,0*-DA-Naph)s, which were obtained after UV irradiation for 10 s. When the *m* value increased, the peak position of the bands shifted to a longer wavelength region; for example, from $\lambda_{max} = 560$ nm for $m = 4$ to $\lambda_{max} = 630$ nm for $m = 16$. Furthermore, the clear even−odd effect of the carbon numbers in the alkyl substituent on the λ_{max} values, as shown in Figure 3b, is different from the results of the layer structures in Figure 2. Figure 3c shows a change in the UV−vis diffusion reflectance spectrum of poly(*5,0*-DA-Naph) during the polymerization, when a low-pressure mercury lamp was used as the light source in order to observe the early stage of polymerization. The peak of the absorption band was observed at 610 nm during the initial polymerization stage. Accordingly, the polymer was first blue. The prolonged UV irradiation resulted in a shift in the band to a shorter wavelength region; namely, the polymer changed from blue to red. For *4,0*-DA-Naph, a color change occurred more rapidly so that we detected no formation of a blue polymer even during the initial stage of the polymerization. The poly(*m,0*-DA-Naph)s having a longer alkyl substituent showed less change in the color during the polymerization, indicating that the chain conformation of the poly(*m,0*-DA-Naph)s with the large *m* value is maintained during the polymerization because of their highly ordered packing structure, while the poly(*m,0*-DA-Naph)s having a shorter alkyl substituent readily change their conformation structures during the polymerization.

Thermochromism of Poly(*m,0*-DA-Naph)s. In order to investigate the temperature dependence of the absorption spectra of poly(*m,0*-DA-Naph)s, photoirradiation of the thin solid films of *m,0*-DA-Naph monomers was carried out for 10 s using a high-pressure mercury lamp, and then the vis absorption spectra were recorded under temperature control by the transmission method without the separation of the resulting polymer and the remaining monomer. The conversion of the monomer to the polymer was estimated to be approximately 5% on the basis of the change in the intensity of the absorption band due to the C≡C bond observed at ca. 2240 cm^{-1} in the IR spectra of the same sample. Upon heating the poly(*m,0*-DA-Naph)s obtained after polymerization, a reversible chromatic change from blue to purple was observed. Changes in the absorption spectrum and in the appearance of poly(*12,0*-DA-Naph) under temperature control in the range of 30−100 °C are shown in Figure 4. The absorption bands of the blue PDA with peaks at 550 and 625 nm at 30 °C gradually shifted to a lower wavelength region during the heating process. Finally, the peaks were observed at 533 and 575 nm at 100 °C. The reversibility of the color change is evident from the spectral change observed in the cooling process. The effect of the alkyl length of the side chain was also examined. Figure 4c shows the shift in the band observed at a longer wavelength for the poly(*m,0*-DA-Naph)s ($m = 4$, 6, 10, and 12) during the heating process. The poly(*m,0*-DA-Naph)s with higher *m* values showed a reversible thermochromism, but the polymers with the shorter alkyl substituents, i.e., the poly(*4,0*-DA-Naph) and poly(6,0-DA-Naph), showed a smaller change.

Regarding the thermochromism of the PDAs, it has been reported that a blue to red thermochromism is associated with the conjugated structure of an alternating ene−yne backbone.[22–24,35] In addition, the electronic property of the polymer main chain is coupled to the conformation and characteristics of the pendant side chain. In the present study, we have further investigated the color change of the poly(*m,0*-DA-Naph)s using temperature-controlled IR spectroscopy, XRD, and DSC measurements. However, no distinctive information was obtained for suggesting any transition due to the conformational change in the polymer chains. In the literature,[23,24] the thermochromism of the PDAs accompanying a slight change in the conformational structure of the methylene groups in the side chain was reported. For example, a gauche conformation is favored at a low temperature while a trans conformation predominantly occurs above the transition temperature. These structural changes can be monitored by Raman spectroscopy but are hardly detected in the IR spectra. The reversible thermochromic transition of the PDAs containing urethane groups in the side chains has been intensively investigated. Tanaka et al.[23b] demonstrated by the sold-state ^{13}C NMR spectroscopy that the alkyl portions of the side chains of the PDAs have the gauche conformation in

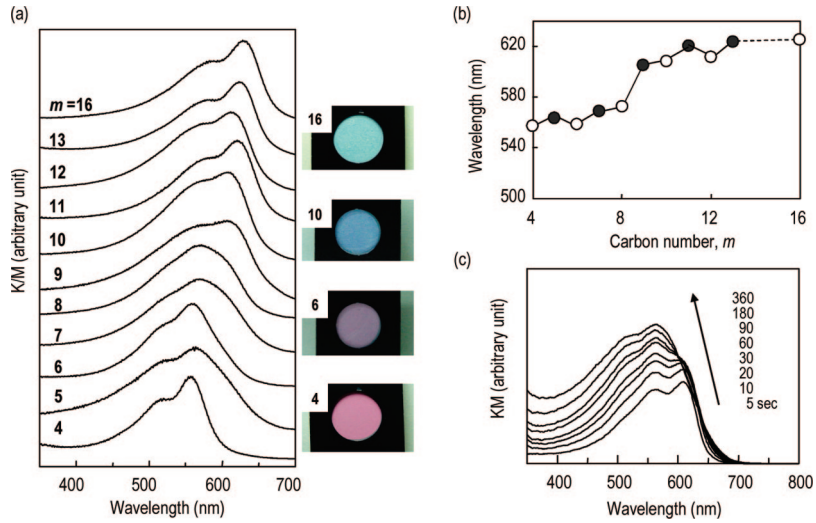

Figure 3. (a) UV−vis diffusion reflectance spectra of *m,0*-DA-Naphs ($m = 4-13$, 16). The *m,0*-DA-Naph was diluted with $MgSO_4$ and the spectra were recorded with an integrating sphere. Polymerization was carried out under photoirradiation using a high-pressure mercury lamp for 10 s. The spectra were recorded by the diffusion reflectance method. (b) Even−odd effect observed for the λ_{max} values depending on the carbon number in the alkyl substituents. (c) Change in the UV−vis diffusion reflectance spectrum of poly(*5,0*-DA-Naph) during UV irradiation using a low-pressure mercury lamp. The vertical axes are represented as KM (Kubelka−Munk) unit in (a) and (c).

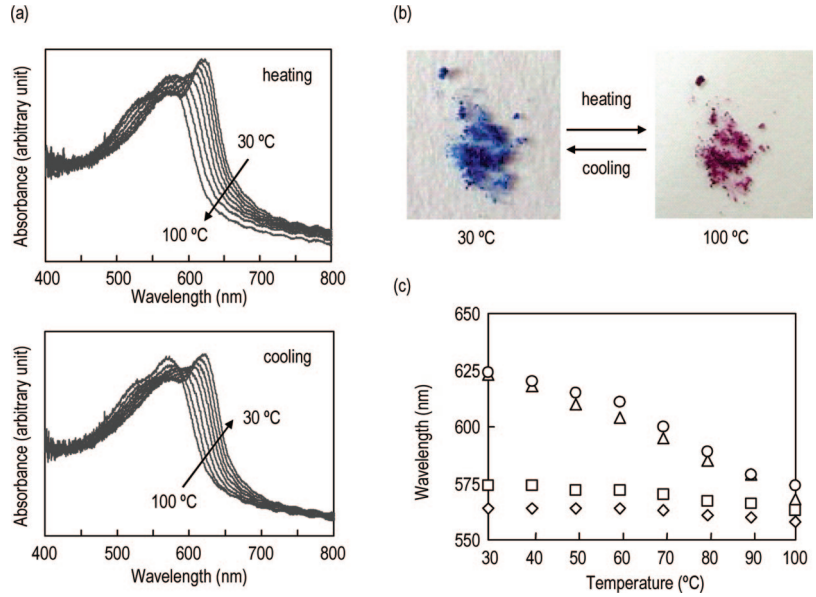

Figure 4. (a) Change in the vis absorption spectrum of poly(*12,0*-DA-Naph) during the heating and cooling processes in the solid film. The solid film was prepared by casting the methanol solution of poly(*12,0*-DA-Naph) on a glass plate and dried at room temperature. The absorption spectra were determined by the transmission method. (b) Color change in appearance of the powdery crystals. (c) Shift in the peak position for the spectra of poly(*m,0*-DA-Naph)s. $m = 4$ (◇), 6 (□), 10 (Δ), and 12 (○).

the blue polymer, while the trans conformation in the red. The gauche conformation is in a higher conformational energy state than the trans conformation, but the polymer backbone is fixed as the higher energy conformation after polymerization by hydrogen bonding as well as side-chain packing. In the blue polymer, the polymer backbone includes strain. The motion of the side chain allows it to have a different conformation upon heating, resulting in the shift of the absorption spectrum to a lower wavelength region. This relaxation of the methylene unit reversiblly occurs.

Thermochromism of Poly(*12,8*-DA-Naph). To investigate the effect of the alkyl spacer between the main chain and the 2D hydrogen bond networks, we prepared *12,8*-DA-Naph. The *12,8*-DA-CO_2H, which is the precursor acid for *12,8*-DA-Naph, also readily produces the blue poly(*12,8*-DA-CO_2H). Mino et al.[11a] reported a reversible change in the absorption spectrum of poly(*12,8*-DA-CO_2H) under highly limited temperature conditions. The peak of the absorption was observed at 650 nm at room temperature and reversibly shifted to 630 nm at 50 °C. Further heating resulted in an irreversible spectral change, namely, $\lambda_{max} = 540$ nm at 60 °C. Thus, the temperature range for the observation of a reversible color change was quite narrow. In the present study, we revealed the chromatic behavior of poly(*12,8*-DA-Naph) as the ammonium salt derivative.

The polymerization of *12,8*-DA-Naph easily occurred under UV irradiation and gave the blue poly(*12,8*-DA-Naph) ($\lambda_{max} =$ 660 nm at 30 °C). The poly(*12,8*-DA-Naph) showed a reversible color change in a broader temperature range. A reversible change was observed between blue and purple in the temperature range of 30−70 °C ($\lambda_{max} = 644$ nm at 70 °C), as shown in Figure 5. An irreversible change occurred upon heating over 70 °C. The spectrum gradually shifted to a shorter wavelength region during the heating process from 30 to 70 °C, and then a discontinuous shift was observed over 70 °C; a new peak began to appear

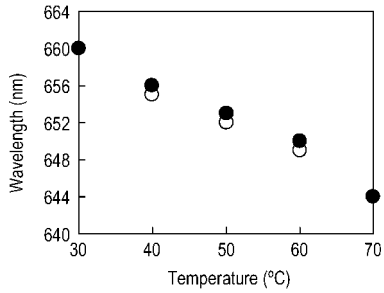

Figure 5. Change in the peak in the vis absorption spectrum of poly(*12,8*-DA-Naph) in the solid state. The open and closed circles indicate the data collected during the cooling and the heating processes, respectively. The absorption spectra were determined by the transmission method.

around 540 nm. Finally, the peaks of the bands were observed at 510 and 550 nm at 100 °C, and the color changed to red. When the temperature-controlled IR measurement was carried out, no change in the structure of the alkyl chain was observed below 80 °C, but broadening of the CH stretching and rocking vibrations were observed at a higher temperature. This suggests that the fluctuation of the alkyl side chain reversibly occurs, but the polymer chains cannot recover their original conformation.

Thus, the introduction of the 2D hydrogen bond networks of the naphthylmethylammonium carboxylates expanded the range for the reversible color change compared to the precursor acid. This fact supports the importance of the 2D hydrogen bond networks included in the PDAs for maintaining the ordered structure of the conjugated main chain. A difference in the thermochromic properties of poly(*m,0*-DA-Naph)s and poly(*m,n*-DA-Naph)s is accounted for by the position of the hydrogen bond networks.

Extension of π-Conjugated System. In the literature,[36–41] few studies on the polymerization of directly phenyl-substituted DA monomers have been reported. One of the reasons is the low reactivity of DA monomers with such a rigid structure for the solid-state polymerization reactivity. Indeed, 1,4-diphenyldiacetylene undergoes no polymerization in the solid state. When the phenyl moieties were modified with any substituents, the polymerization occurred and the resulting PDAs showed enhanced optical and electrical properties. In the present study, DAs with a 4-carboxyphenyl substituent, *m,Ph*-DA-CO_2Hs, were synthesized and also transformed to the corresponding ammonium DA derivatives, *m,Ph*-DA-Naphs. The PDAs obtained by the polymerization are expected to have a highly π-conjugated ene−yne backbone, at which a phenylene group is directly bound to. Eventually, *m,Ph*-DA-CO_2Hs and *m,Ph*-DA-Naphs were isolated as polycrystalline powders, and the both series of monomers were found to undergo solid-state polymerization, while Ogawa et al.[40] previously reported that the LB film of *m,Ph*-DA-CO_2H having a short alkyl chain ($m = 5$ and 6) did not undergo polymerization.

Both *m,Ph*-DA-Naphs and *m,Ph*-DA-CO_2Hs slowly underwent solid-state polymerization under photoirradiation and provided polymers exhibiting a strong absorption in the visible region. This is contrast to the fast polymerization of *m,0*-DA-Naphs and *12,8*-DA-Naph even under the irradiation conditions with a scattered light in a room. The blue and pale green polymers were produced during the UV irradiation of the *m,Ph*-DA-Naph and *m,Ph*-DA-CO_2H crystals, respectively. The polymerization was also confirmed by a change in the IR spectrum. For example, the peak intensity of a stretching vibration band due to a diacetylene bond observed at 2243 cm^{-1} gradually decreased, and simultaneously, another kind of acetylenic stretching band at 2197 cm^{-1} increased during the photoirradiation of *16,Ph*-DA-CO_2H. The results of the γ-radiation polymerization of *m,Ph*-DA-Naphs and *m,Ph*-DA-CO_2Hs are summarized in Table 1, together with the maximum absorption wavelength in their absorption spectra. As a result, it was revealed that the poly(*10,Ph*-DA-Naph) and poly(*12,Ph*-DA-Naph) were partly soluble in THF at ambient temperature. The soluble part was analyzed by GPC to determine the molecular weight of the resulting polymers ($M_n = (3.2-4.9) \times 10^4$). The poly(*16,Ph*-DA-Naph) with a longer alkyl substituent was insoluble in THF. The poly(*m,Ph*-DA-CO_2H)s were insoluble in many organic solvents, including toluene, chloroform, THF, and dimethyl sulfoxide. The conversion to the polymers was gravimetrically determined after the isolation by removing the unreacted monomers with THF. The polymer yields were 7−15% after the γ-radiation at a dose of 200 kGy ($=2 \times 10^7$ rad). Even if irradiated at an extremely high radiation dose of 1000 kGy ($=10^8$ rad), the polymer yield was only 23% for *16,Ph*-DA-CO_2H. This is contrast to the fact that the other topochemically polymerizable diyne and diene monomers produce the corresponding polymers in a high yield under similar radiation conditions.[42,43]

Table 1. γ-Radiation Polymerization of *m,Ph*-DA-Naphs and *m,Ph*-DA-CO_2Hs and Characterization of the Resulting Polymers

compound	yield[a] (%)	λ_{max}[b] (nm)	$M_n \times 10^{-4}$	M_w/M_n
10,Ph-DA-Naph	*c*, *d*	552, 593	3.2	3.2
12,Ph-DA-Naph	*c*, *d*	543, 585	4.9	6.5
16,Ph-DA-Naph	15	556, 595	*d*	*d*
8,Ph-DA-CO_2H	*d*	600, 670	*d*	*d*
10,Ph-DA-CO_2H	8	606, 670	*d*	*d*
12,Ph-DA-CO_2H	11	610, 673	*d*	*d*
16,Ph-DA-CO_2H	7 (23)[e]	616, 676	*d*	*d*

[a] The polymerization was carried out under γ-radiation at a dose of 200 kGy. The polymer yield was gravimetrically determined after removing the unreacted monomer with THF for poly(*m,Ph*-DA-Naph)s and by filtration of the dispersed solution of the polymerization mixture in THF using a micropore filter for poly(*m,Ph*-DA-CO_2H)s. [b] The vis absorption spectra were determined by the transmission method using the obtained samples without removing the unreacted monomer. [c] The resulting polymer was partly soluble in THF. [d] Not determined. [e] Radiation dose of 1000 kGy.

From the powder X-ray diffraction data of *m,Ph*-DA-Naphs and *m,Ph*-DA-CO_2Hs, the both monomers are estimated to have a molecular packing structure similar to that for *m,0*-DA-Naphs. In Figure 2, the *d*-spacing values are plotted against to the carbon numbers of the alkyl substituent for the *m,Ph*-DA-Naph and *m,Ph*-DA-CO_2H series. Interestingly, the slope of the lines for the *m,Ph*-DA-Naphs and *m,Ph*-DA-CO_2Hs was identical to that for *m,0*-DA-Naphs, in which the alkyl chains are stacked with the tilt angle of 43°. Consequently, the diacetylene moieties are stacked in a columnar structure with a similar stacking distance and angle for the phenyl-substituted PD monomers. Furthermore, this result indicates that the carboxylic acid derivatives can be readily arranged in the stacking structure appropriate for the polymerization, similar to the alkadiynoic acids including *12,8*-DA-CO_2H. The low polymerization reactivity of these phenyl-substituted DA monomers is assumed to be due to the difficulty of the conformational change of the phenyl substituents, which are directly connected to the reacting center. No single crystal structure data are available for the polymerizable phenyl-substituted DA monomers in the present study and literature.

Thermochromism of Poly(*m,Ph*-DA-Naph)s. The poly(*m,Ph*-DA-Naph)s showed a thermally reversible chromatic change upon heating, as shown in Figure 6. The spectrum of the blue poly(*16,Ph*-DA-Naph) at 30 °C consisted of bands with peaks at 555 and 595 nm and the type of spectral change during heating was different from that of the poly(*m,0*-DA-Naph)s. The intensity of the absorption at the longer wavelength gradually

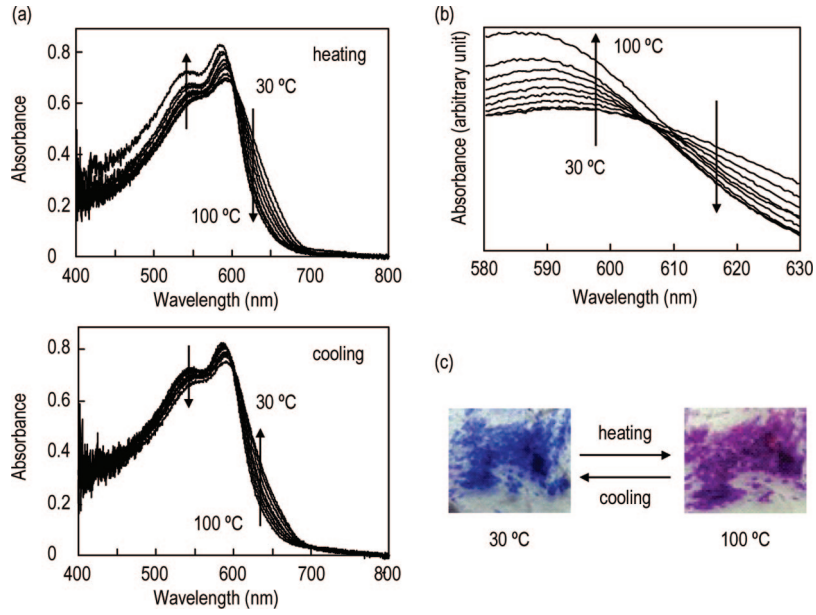

Figure 6. (a) Change in the vis absorption spectrum of poly(*16,Ph*-DA-Naph) during the heating and cooling processes in the solid state. The absorption spectra were determined by the transmission method. (b) Expansion spectra. (c) Change in the color of the polymer.

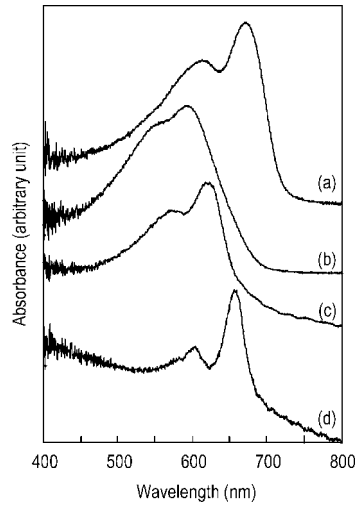

Figure 7. Vis absorption spectra of (a) poly(*16,Ph*-DA-CO_2H), (b) poly(*16,Ph*-DA-Naph), (c) poly(*12,0*-DA-Naph), and (d) poly(*12,8*-DA-Naph) obtained photopolymerization in the solid state. The absorption spectra were determined by the transmission method.

decreased, and simultaneously the intensity of the shorter band increased with an isosbestic point at 606 nm. No peak shift was observed below 90 °C. The peaks of the absorption bands slightly shifted from 555 and 595 nm to 545 and 587 nm during the temperature change from 90 to 100 °C. Thus, only a small peak shift was observed during the transition of poly(*16,Ph*-DA-Naph), while a clear spectral shift was observed in the case of poly(*m,0*-DA-Naph)s. This result implies that the thermochromism of poly(*16,Ph*-DA-Naph) is closely related to the switching of the conjugation between the aromatic substituent and the conjugated polymer backbone. The observation of small deviation from the isosbestic point near 100 °C is attributed to the conformational change in the polymer backbone. For the poly(*m,Ph*-DA-Naph)s, their conjugated polymer chain conformation is fixed by their robust structure of the 2D hydrogen bond networks, which are similar to those for the poly(*m,0*-DA-Naph)s. In addition, the steric hindrance of the aromatic rings introduces the torsion of the polymer backbone of the poly(*m,Ph*-DA-Naph)s, leading to the absorption bands at a wavelength lower than those for the poly(*m,0*-DA-Naph) and poly(*12,8*-DA-Naph) (Figure 7).

On the other hand, the absorption of the poly(*m,Ph*-DA-CO_2H)s appeared at ca. 610 and 670 nm for the bands due to the conjugating main chain and their exciton interactions. The wavelength of the absorption band of poly(*16,Ph*-DA-CO_2H) is much higher than those for the other PDAs investigated in the present study and also reported in the literature.[4,6–8] The absorption bands slightly shifted to a longer wavelength region with an increase in the alkyl chain length (Table 1). The longer conjugating length in the main chain of poly(*m,Ph*-DA-CO_2H)s are due to the effective conjugation with a 4-carboxyphenyl group in the side chain. Previously, Ogawa et al.[40] reported that the LB film of the meta-derivatives of the PDA with a similar structure ($m = 10$) has an absorption maxima at 600 and 640 nm. This indicates that the *p*-benzoic acid derivatives have a longer conjugated length than the meta-isomers. More detailed chromatic and structural properties of the poly(*m,Ph*-DA-CO_2H)s are now under investigation.

Conclusions

In the present study, we investigated the molecular packing structure and the solid-state polymerization behavior of diacetylene compounds containing a naphthylmethylammonium carboxylate group in the side chain, which makes robust and 2D hydrogen bond networks. For the *m,0*-DA-Naphs, all the naphthylmethylammonium salts were isolated as colorless crystals. The position of the absorption bands for the poly(*m,0*-DA-Naph)s, obtained by the solid-state polymerization under UV irradiation, depended on the alkyl chain length of the side chain. The poly(*m,0*-DA-Naph)s showed a reversible color change in a wide temperature range upon heating. This is in contrast to the partly reversible color change of the poly(*12,8*-DA-Naph). This difference is due to the position of the 2D hydrogen bond network, which supports the conjugated backbone structure. The polymerization of the *m,Ph*-DA-Naphs, of which the acetylene moiety is directly substituted by an aromatic ring, also occurred and provided PDAs with absorption characteristics different from those of the poly(*m,0*-DA-Naph)s. The poly(*16,Ph*-DA-Naph) also showed a reversible color change upon heating, but the mechanism is different from that of the poly(*m,0*-DA-Naph)s. The thermochromism of poly(*16,Ph*-DA-

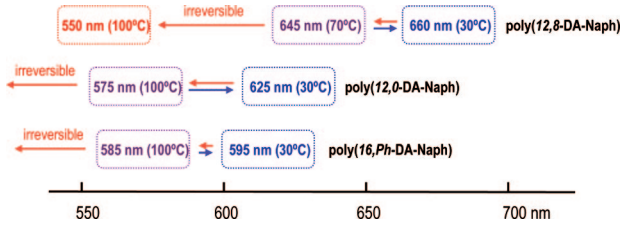

Figure 8. Summary of the effect of polymer structures on the thermochromic behavior for PDAs. The wavelength values in this figure indicate the maximum value of the absorption band at each temperature.

Naph) is probably based on the conformational changes in the aromatic substituent and the conjugating backbone structure.

Figure 8 shows a summary of the color changes of the PDAs investigated in the present study. The chromatic behaviors of the PDAs are classified into several states. The polymerization of the DAs proceeds in the solid state under kinetic control, and as a result, a strained polymer is produced during the initial stage of the polymerization. During the polymerization, such a strain is gradually released and this step is irreversible. Upon heating of the polymer a visible absorption band shifted to a shorter wavelength region and transformed into another state, which shows different chromatic properties. This process is due to the thermal fluctuation of the side chain, resulting in the torsion structure of the conjugated backbones. A transformation between these states is reversible. Furthermore, a more disordered structure exists at a higher temperature, accompanied by a discontinuous spectral change. This transition is no longer reversible. It has also been revealed that poly(*16,Ph*-DA-Naph) shows a reversible thermal color change based on the conformational changes of the aromatic substituent and the conjugating backbone, differing from the other polymers, i.e., poly(*12,8*-DA-Naph) and poly(*12,0*-DA-Naph).

Acknowledgment. This work was supported by Grants-in-Aid for Scientific Research on Priority Areas "Super-Hierarchical Structures" (Area No. 446, No. 19022032) from the Ministry of Education, Culture, Sports, Science and Technology (MEXT) of Japan. We gratefully thank Prof. Kunio Oka, Osaka Prefecture University, for his kind assistance with the γ-radiation experiment.

References and Notes

(1) Skothem, T. A., Reynolds, J. R., Eds.; *Handbook of Conjugating Polymers*, 3rd ed.; CRC Press: New York, 2007.
(2) (a) Shirakawa, H. *Angew. Chem., Int. Ed.* **2001**, *40*, 2574. (b) MacDiarmid, A. G. *Angew. Chem., Int. Ed.* **2001**, *40*, 2581. (c) Heeger, A. J. *Angew. Chem., Int. Ed.* **2001**, *40*, 2591.
(3) (a) Kraft, A.; Grimsdale, A. C.; Holmes, A. B. *Angew. Chem., Int. Ed.* **1998**, *37*, 402. (b) McCullough, R. D. *Adv. Mater.* **1998**, *10*, 93. (c) Martin, R. E.; Diederich, F. *Angew. Chem., Int. Ed.* **1999**, *38*, 1350. (d) Bunz, U. H. F. *Chem. Rev.* **2000**, *100*, 1605. (e) Dimitrakopoulos, C. D.; Malenfant, P. R. L. *Adv. Mater.* **2002**, *14*, 99. (f) Scherf, U.; List, E. J. W. *Adv. Mater.* **2002**, *14*, 477. (g) Yokozawa, T. *Macromolecules* **2007**, *40*, 4093. (h) Morisaki, Y.; Chujo, Y. *Angew. Chem., Int. Ed.* **2006**, *45*, 2.
(4) (a) Chemla, D. S., Zyss, J., Eds.; *Nonlinear Optical Properties of Organic Molecules and Crystals*; Academic Press: New York, 1987. (b) Sarkar, A.; Okada, S.; Matsuzawa, H.; Matsuda, H.; Nakanishi, H. *J. Mater. Chem.* **2000**, *10*, 819.
(5) (a) Swager, T. M. *Acc. Chem. Res.* **1998**, *31*, 201. (b) Thomas III, S. W.; Joly, G. D.; Swager, T. M. *Chem. Rev.* **2007**, *107*, 1339. (c) Kim, J.-M. *Macromol. Rapid Commun.* **2007**, *28*, 1191.
(6) Zuilhof, H.; Barentsen, H. M.; van Dijk, M.; Sudhölter, E. J. R.; Hoofman, R. J. O. M.; Siebbeles, L. D. A.; de Haas, M. P.; Warman, J. M. *Supramolecular Photosensitive and Electroactive Materials*; Nalwa, H. S., Ed.; Academic Press: New York, 2001, p 339, and the references cited therein.
(7) (a) Wegner, G. Z. *Z. Naturforsch.* **1969**, *24b*, 824. (b) Wegner, G. *Pure Appl. Chem.* **1977**, *49*, 443. (c) Enkelmann, V. *Adv. Polym. Sci.* **1984**, *63*, 91. (d) Tieke, B. *Adv. Polym. Sci.* **1985**, *71*, 79.
(8) Recent reviews: (a) Ahn, D. J.; Kim. J.-M. *Acc. Chem. Res.* **2008**, *41*, 805. (d) Sada, K.; Takeuchi, M.; Fujita, N.; Numata, M.; Shinkai, S. *Chem. Soc. Rev.* **2007**, *36*, 415.
(9) Okada, S.; Peng, S.; Spevak, W.; Charych, D. *Acc. Chem. Res.* **1998**, *31*, 229.
(10) (a) Charych, D. H.; Nagy, J. O.; Spevak, W.; Bednarski, M. D. *Science* **1993**, *261*, 585. (b) Reichert, A.; Nagy, J. O.; Spevak, W.; Charych, D. *J. Am. Chem. Soc.* **1995**, *117*, 829. (c) Lio, A.; Reichert, A.; Ahn, D. J.; Nagy, J. O.; Salmeron, M.; Charych, D. H. *Langmuir* **1997**, *13*, 6524.
(11) (a) Mino, N.; Tamura, H.; Ogawa, K. *Langmuir* **1991**, *7*, 2336. (b) Deckert, A. A.; Home, J. C.; Valentine, B.; Kernan, L.; Fallon, L. *Langmuir* **1995**, *11*, 643. (c) Carpick, R. W.; Mayer, T. M.; Sasaki, D. Y.; Burns, A. R. *Langmuir* **2000**, *16*, 4639.
(12) (a) Ahn, D. J.; Chae, E. H.; Lee, G. S.; Shim, H. Y.; Chang, T. E.; Ahn, K. D.; Kim, J.-M. J. *Am. Chem. Soc.* **2003**, *125*, 8976. (b) Kim, J. -M.; Lee, J. S.; Choi, H.; Sohn, D.; Ahn, D. J. *Macromolecules* **2005**, *38*, 9366. (c) Lee, S.; Kim, J.-M. *Macromolecules* **2007**, *40*, 9201.
(13) Park, B. H.; Lee, J. S.; Choi, H.; Ahn, D. J.; Kim, J. -M. *Adv. Funct. Mater.* **2007**, *17*, 3447.
(14) (a) Peng, H.; Tang, J.; Pang, J.; Chen, D.; Yang, L.; Ashbaugh, H. S.; Brinker, C. J.; Yang, Z.; Lu, Y. J. *Am. Chem. Soc.* **2005**, *127*, 12782. (b) Peng, H. S.; Tang, J.; Yang, L.; Pang, J. B.; Ashbaugh, H. S.; Brinker, C. J.; Yang, Z. Z.; Lu, Y. F. *J. Am. Chem. Soc.* **2006**, *128*, 5304.
(15) (a) Lu, Y.; Yang, Y.; Sellinger, A.; Lu, M.; Huang, J.; Fan, H.; Haddad, R.; Lopez, G.; Burns, A. R.; Sasaki, D. Y.; Shelnutt, J.; Brinker, C. J. *Nature (London)* **2001**, *410*, 913. (b) Yang, Y.; Lu, Y.; Lu, M.; Huang, J.; Haddad, R.; Xomeritakis, G.; Liu, N.; Malanoski, A. P.; Sturmayr, D.; Fan, H.; Sasaki, D. Y.; Assink, R. A.; Shelnutt, J. A.; Swol, F.; Lopez, G. P.; Burns, A. R.; Brinker, C. J. J. *J. Am. Chem. Soc.* **2003**, *125*, 1269.
(16) Dautel, O. J.; Robitzer, M.; Lère-Porte, J. -P.; Serein-Spirau, F.; Moreau, J. J. E. *J. Am. Chem. Soc.* **2006**, *128*, 16213.
(17) Lam, J. W. Y.; Tang, B. Z. *Acc. Chem. Res.* **2005**, *38*, 745.
(18) (a) Yoshino, K.; Morita, S.; Yin, X. H.; Kawai, T. *Jpn. J. Appl. Phys* **1993**, *32*, L547. (b) K.Tachibana, H.; Hosaka, N.; Tokura, Y. *Macromolecules* **2001**, *34*, 1823.
(19) (a) Gelinck, G. H.; Warman, J. M.; Staring, E. G. J. *J. Phys. Chem.* **1996**, *100*, 5485. (b) Chen, S. A.; Chang, E. C. *Macromolecules* **1998**, *31*, 4899. (c) Nakanishi, N.; Tada, K.; Onoda, M. *Jpn. J. Appl. Phys. Part 1* **2000**, *39*, 1913.
(20) Li, X. G.; Zhou, H. J.; Huang, M. R. *Polymer* **2005**, *46*, 1523.
(21) Miller, R. D.; Michl, J. *Chem. Rev.* **1989**, *89*, 1359.
(22) (a) Chance, R. R.; Baughman, R. H.; Muller, H.; Echhart, J. G. *J. Chem. Phys.* **1977**, *67*, 3616. (b) Wenz, G.; Müller, M. A.; Schmit, M.; Wegner, G. *Macromolecules* **1984**, *17*, 837. (c) Orchard, B. J.; Tripathy, S. K. *Macromolecules* **1986**, *19*, 1844. (d) Kuriyama, K.; Kikuchi, H.; Oishi, Y.; Kajiyama, T. *Langmuir* **1996**, *11*, 3536. (e) Saito, A.; Urai, Y.; Itoh, K. *Langmuir* **1996**, *12*, 3938. (f) Huo, Q.; Russev, S.; Hasegawa, T.; Nishijo, J.; Umemura, J.; Puccetti, G.; Russell, K. C.; Leblanc, R. M. *J. Am. Chem. Soc.* **2000**, *122*, 7890.
(23) (a) Galambos, A. F.; Stockton, W. B.; Koberstein, J. T.; Sen, A.; Weiss, R. A.; Russell, T. P. *Macromolecules* **1987**, *20*, 3094. (b) Tanaka, H.; Gomez, M. A.; Tonelli, A. E.; Thakur, M. *Macromolecules* **1989**, *22*, 1208.
(24) (a) Rubner, M. F.; Sandman, D. J.; Velazquez, *Macromolecules* **1987**, *20*, 1296. (b) Downey, M. J.; Hamill, G. P.; Rubner, M.; Sandman, D. J.; Velazques, C. S. *Makromol. Chem.* **1988**, *189*, 1199.
(25) (a) Matsumoto, A.; Sada, K.; Tashiro, K.; Miyata, M.; Tsubouchi, T.; Tanaka, T.; Odani, T.; Nagahama, S.; Tanaka, T.; Inoue, K.; Saragai, S.; Nakamoto, S. *Angew. Chem., Int. Ed.* **2002**, *41*, 2502. (b) Matsumoto, A. *Polym. J.* **2003**, *35*, 93. (c) Matsumoto, A. *Top. Curr. Chem.* **2005**, *254*, 263.
(26) (a) Matsumoto, A.; Odani, T.; Chikada, M.; Sada, K.; Miyata, M. *J. Am. Chem. Soc.* **1999**, *121*, 11122. (b) Matsumoto, A.; Nagahama, S.; Odani, T. *J. Am. Chem. Soc.* **2000**, *122*, 9109. (c) Matsumoto, A.; Nagahama, S. *J. Am. Chem. Soc.* **2001**, *123*, 12176. (d) Nagahama, S.; Inoue, K.; Sada, K.; Miyata, M.; Matsumoto, A. *Cryst. Growth Des.* **2003**, *3*, 247.
(27) (a) Sada, K.; Inoue, K.; Tanaka, T.; Tanaka, A.; Epergyes, A.; Nagahama, S.; Matsumoto, A.; Miyata, M. *J. Am. Chem. Soc.* **2004**, *126*, 1764. (b) Sada, K.; Inoue, K.; Tanaka, T.; Epergyes, A.; Tanaka, A.; Tohnai, N.; Matsumoto, A.; Miyata, M. *Angew. Chem., Int. Ed.* **2005**, *44*, 7059.
(28) Brandsma, L. *Preparative Acetylenic Chemistry*, 2nd ed.; Elsevier: Amsterdam, 1988.
(29) Yashima, E.; Matsushima, T.; Okamoto, Y. *J. Am. Chem. Soc.* **1997**, *119*, 6345.
(30) For the single-crystal structure of *4,0*-DA-Naph: (a) Matsumoto, A.; Matsumoto, A.; Kunisue, T.; Tanaka, A.; Tohnai, N.; Sada, K.; Miyata, M. *Chem. Lett.* **2004**, *33*, 96.

(31) (a) Matsumoto, A.; Odani, T.; Sada, K.; Miyata, M.; Tashiro, K. *Nature (London)* **2000**, *405*, 328. (b) Matsumoto, A.; Oshita, S.; Fujioka, D. *J. Am. Chem. Soc.* **2002**, *124*, 13749.
(32) (a) Yang, H. C.; Aoki, K.; Hong, H. -G.; Sackett, D. E.; Arendt, M. F.; Yau, S. -L.; Bell, C. M.; Mallouk, T. E. *J. Am. Chem. Soc.* **1993**, *115*, 11855. (b) Alberti, G.; Costantino, U.; Dionigi, C.; Murcia-Mascaros, S.; ViVani, R. *Supramol. Chem.* **1995**, *6*, 29. (c) Katoh, K.; Shichi, T.; Takagi, K. *Chem. Lett.* **1999**, 117. (d) Takagi, K.; Saito, N.; Shichi, T.; Sawaki, Y. *Chem. Lett.* **1999**, 275. (e) O'Hare, D.; Evans, J. S. O.; Fogg, A.; O'Brien, S. *Polyhedron* **2000**, *19*, 297.
(33) (a) Boese, R.; Weiss, H. -C.; Bläser, D. *Angew. Chem., Int. Ed.* **1999**, *38*, 988. (b) Thalladi, V. R.; Boese, R.; Weiss, H. -C. *Angew. Chem., Int. Ed.* **2000**, *39*, 918. (c) Thalladi, V. R.; Nüsse, M.; Boese, R. *J. Am. Chem. Soc.* **2000**, *122*, 9227.
(34) Kitaigorodsky, A. I. *Molecular Crystals and Molecules*; Academic Press: New York, 1973.
(35) (a) Exarhos, G. J.; Risen, W. M., Jr.; Baughman, R. H. *J. Am. Chem. Soc.* **1976**, *98*, 481. (b) Chance, R. R.; Baughman, R. H.; Müller, H.; Eckhardt, C. J. *J. Chem. Phys.* **1977**, *67*, 3616. (c) Eckhardt, H.; Eckhardt, C. J.; Yee, K. C. *J. Chem. Phys.* **1979**, *70*, 5498. (d) Hoofman, R. J. O. M.; Gelinck, G. H.; Siiebbeles, L. D. A.; de Haas, M. P.; Warman, J. M.; Bloor, D. *Macromolecules* **2000**, *33*, 9289. (e) Lee, D. -C.; Sahoo, S. K.; Cholli, A. L.; Sandman, D. J. *Macromolecules* **2002**, *35*, 4347. (f) Wang, X. Y.; Whitten, J. E.; Sandman, D. J. *J. Chem. Phys.* **2007**, *126*184905.
(36) Baughman, R. H. *J. Appl. Phys.* **1972**, *43*, 4362.
(37) Kojima, Y.; Matsuoka, T.; Takahashi, H. *J. Mater. Sci. Lett.* **1996**, *15*, 539.
(38) (a) Okada, S.; Ohsugi, M.; Masaki, A.; Matsuda, H.; Takaragi, S.; Nakanishi, H. *Mol. Cryst. Liq. Cryst.* **1990**, *183*, 81. (b) Sarkar, A.; Okada, S.; Nakanishi, H.; Matsuda, H. *Macromolecules* **1998**, *31*, 9174.
(39) Okuno, T.; Izuoka, A.; Ito, T.; Kubo, S.; Sugawara, T.; Sato, N.; Sugawara, Y. *J. Chem. Soc., Perkin Trans. 2* **1998**, 889.
(40) (a) Burillo, G. ; Torres, S.; Ogawa, T. *J. Appl. Polym. Sci., Appl. Polym. Symp.* **1991**, *49*, 1. (b) Carréon, M.; Burillo, G. ; Agabekov, V.; Ogawa, T. *Polym. J.* **1997**, *29*, 103.
(41) Chan, Y. -H.; Lin, J. -T.; Chen, I -W. P.; Chen, C. -H. *J. Phys. Chem. B* **2005**, *109*, 19161.
(42) (a) Matsumoto, A.; Katayama, K.; Odani, T.; Oka, K.; Tashiro, K.; Saragai, S.; Nakamoto, S. *Macromolecules* **2000**, *33*, 7786. (b) Matsumoto, A.; Chiba, T.; Odani, T.; Oka, K. *Macromolecules* **2003**, *36*, 2573. (c) Mori, Y.; Chiba, T.; Odani, T.; Matsumoto, A. *Cryst. Growth Des.* **2007**, *7*, 1356.
(43) Dei, S.; Matsumoto, A.; Matsumoto, A. *Macromolecules* **2008**, *41*, 2467.

MA800824S